

**RESEARCH ARTICLE**

# Different reactivities of $\text{H}_3\text{O}^+(\text{H}_2\text{O})_n$ with unsaturated and saturated aldehydes: ligand-switching reactions govern the quantitative analytical sensitivity of SESI-MS

Patrik Španěl<sup>1</sup>  | Kseniya Dryahina<sup>1</sup>  | Maroua Omezzine Gnioua<sup>1,2</sup>  | David Smith<sup>1</sup> 

<sup>1</sup>J. Heyrovsky Institute of Physical Chemistry of the Czech Academy of Sciences, Prague, Czechia

<sup>2</sup>Department of Surface and Plasma Science, Faculty of Mathematics and Physics, Charles University, Prague, Czech Republic

**Correspondence**

Patrik Španěl, J. Heyrovsky Institute of Physical Chemistry of the Czech Academy of Sciences, Dolejškova 3, Prague 8, 18223, Czechia.

Email: [spanel@jh-inst.cas.cz](mailto:spanel@jh-inst.cas.cz)

**Funding information**

Grantová Agentura České Republiky, Grant/Award Number: 21-25486S.

**Rationale:** The detection sensitivity of secondary electrospray ionisation mass spectrometry (SESI-MS) is much lower for saturated aldehydes than for unsaturated aldehydes. This needs to be understood in terms of gas phase ion-molecule reaction kinetics and energetics to make SESI-MS analytically more quantitative.

**Methods:** Parallel SESI-MS and selected ion flow tube mass spectrometry (SIFT-MS) analyses were carried out of air containing variable accurately determined concentrations of saturated (C5, pentanal; C7, heptanal; C8 octanal) and unsaturated (C5, 2-pentenal; C7, 2-heptenal; C8, 2-octenal) aldehyde vapours. The influence of the source gas humidity and the ion transfer capillary temperature, 250 and 300°C, in a commercial SESI-MS instrument was explored. Separate experiments were carried out using SIFT to determine the rate coefficients,  $k_{73}$ , for the ligand-switching reactions of the  $\text{H}_3\text{O}^+(\text{H}_2\text{O})_3$  ions with the six aldehydes.

**Results:** The relative slopes of the plots of SESI-MS ion signal against SIFT-MS concentration were interpreted as the relative SESI-MS sensitivities for these six compounds. The sensitivities for the unsaturated aldehydes were 20 to 60 times greater than for the corresponding C5, C7 and C8 saturated aldehydes. Additionally, the SIFT experiments revealed that the measured  $k_{73}$  are three or four times greater for the unsaturated than for the saturated aldehydes.

**Conclusions:** The trends in SESI-MS sensitivities are rationally explained by differences in the rates of the ligand-switching reactions, which are justified by theoretically calculated equilibrium rate constants derived from thermochemical density functional theory (DFT) calculations of Gibb's free energy changes. The humidity of SESI gas thus favours the reverse reactions of the saturated aldehyde analyte ions, effectively suppressing their signals in contrast to their unsaturated counterparts.

This is an open access article under the terms of the [Creative Commons Attribution-NonCommercial](https://creativecommons.org/licenses/by-nc/4.0/) License, which permits use, distribution and reproduction in any medium, provided the original work is properly cited and is not used for commercial purposes.

© 2023 The Authors. *Rapid Communications in Mass Spectrometry* published by John Wiley & Sons Ltd.

## 1 | INTRODUCTION

Secondary electrospray ionisation (SESI)<sup>1,2</sup> used for gas phase analysis involves the reactions of trace volatile molecular gases with ions formed in a spray of charged nanodroplets emitted from a needle capillary held at a high positive or negative potential into air or nitrogen at or near atmospheric pressure.<sup>3</sup> The hydrated hydronium reagent ions,  $\text{H}_3\text{O}^+(\text{H}_2\text{O})_n$ , react with analyte molecules present in the gaseous sample introduced in the surrounding air/nitrogen. This is the basis of a very sensitive analytical technique when coupled to a mass spectrometer, SESI-MS. The reagent cluster ions formed in the gas phase are in a thermodynamic equilibrium distribution that is dependent on the surrounding gas humidity and temperature.<sup>4</sup>

We realised that there is some room to improve the understanding of the underlying ion chemistry in this area, thus we began to investigate this in a systematic way. Our first investigation<sup>4</sup> involved the reagent cluster ion distribution in a SESI-MS instrument operated in near-atmospheric pressure at 30°C and absolute humidity near 1%. This revealed that reagent cluster ions  $\text{H}_3\text{O}^+(\text{H}_2\text{O})_n$  for  $n > 4$  were available to react by ligand-switching reactions<sup>4-6</sup> with reagent gases, M, which led to the conclusion that the commonly assumed exothermic proton transfer to produce  $\text{MH}^+$  analyte ions<sup>7,8</sup> could not be the dominant reaction process. In fact, ligand switching is the dominant gas phase ion-molecule reaction process occurring in the SESI ion spray. The mechanism of the SESI is currently a subject of further active investigation; it was recently suggested that whilst the initial ionisation process involved is “soft,” i.e., it produces ions with low internal energy, analyte ion collisional fragmentation can occur during their transfer from the atmospheric ionisation region to the mass spectrometer.<sup>5,9</sup>

Reagent and analyte ions are formed in relatively high-pressure gas and must be transported to a necessarily low-pressure analytical mass spectrometer. Conventionally, in electrospray ionisation (ESI), this is achieved in one of two ways. First, the ion source can be coupled to the MS chamber by an ion transfer capillary tube and a gas ( $\text{N}_2$  or air) flow sufficient for efficient ion transport whilst the MS chamber is pumped to a suitably low pressure. Reagent and analyte ion currents are decreased by diffusive loss to the capillary walls, which in practice is not a limiting factor given the powers of the ESI ion source. Heating the transfer capillary assists dissociation (desolvation) of hydrated ions. This is a commonly used configuration for SESI,<sup>3,7,10-12</sup> as described in a previous paper,<sup>4</sup> which also showed the equilibrium distributions of  $\text{H}_3\text{O}^+(\text{H}_2\text{O})_n$  ions and their reactions with  $\text{NH}_3$  analyte molecules that displace  $\text{H}_2\text{O}$  ligands from the  $\text{H}_3\text{O}^+(\text{H}_2\text{O})_n$  ions at the collisional rate forming  $\text{NH}_4^+(\text{H}_2\text{O})_m$  ions, which travel through the heated ion transfer capillary losing  $\text{H}_2\text{O}$  molecules. Second, the reagent and analyte ions can be sampled into a low-pressure MS chamber using small apertures for pressure reduction using embedded electric fields, E, to direct the ions into the MS as used in the ZSpray.<sup>5</sup> In this arrangement, collisions of ions with background molecules occur, and by varying the electric fields strengths controlled dissociation of the hydrated reagent ions,  $\text{H}_3\text{O}^+(\text{H}_2\text{O})_n$ , and analyte ions, the hydrates  $\text{MH}^+(\text{H}_2\text{O})_m$ , as derived

from analyte molecules, M, i.e., can be explored prior to the MS sampling. This was examined in a previous paper<sup>5</sup> when it was shown that the E-field strengths and arrangements influence the relative fractions of  $\text{MH}^+$  and its hydrates, which need to be understood to realise quantification of trace gases, M. E-field desolvation resulted in largely the protonated volatile organic compounds (VOCs),  $\text{MH}^+$ , and their monohydrates,  $\text{MH}^+\text{H}_2\text{O}$ . There was a linear response of the ion signal to the measured VOC sample concentration, which provided the instrument sensitivities, S, for 25 VOCs. This study showed very wide variations in S from near-zero to 1 for hydrocarbons, and up to 100, on a relative scale, for polar compounds such as monoketones and unsaturated aldehydes. This needs to be explained if SESI-MS is to be used for accurate analyses of mixtures containing various organic compounds. The most surprising result is that saturated aldehydes were relatively unreactive and, in comparison, unsaturated aldehydes were 11 to 36 times more reactive. Remembering that the actual reaction process in the SESI ion plume is ligand switching between  $\text{H}_3\text{O}^+(\text{H}_2\text{O})_n$  mostly for  $n$  greater than 3, an experiment is required that can explore the switching reactions of these cluster ions with organic vapours.

Fortunately, the Profile 3 selected ion flow tube, SIFT, instrument has the specific purpose of studying ion-molecule reactions. However, it is not easy to inject weakly-bound cluster ions into helium carrier gas and so only a few studies have been conducted.<sup>13,14</sup> The ion cluster  $\text{H}_3\text{O}^+(\text{H}_2\text{O})_3$  at  $m/z$  73 can be made the dominant species in the flow tube by introducing sufficient water vapour to promote its formation from injected  $\text{H}_3\text{O}^+$  at  $m/z$  19.<sup>15,16</sup> For the purpose of the present study, guided by the earlier SESI-MS results, we carried out a SIFT study of the kinetics and energetics of the reactions of  $\text{H}_3\text{O}^+(\text{H}_2\text{O})_3$  with three saturated aldehydes and their analogous unsaturated aldehydes. This required quantum chemical calculations of the thermodynamic parameters  $\Delta H$  and  $\Delta G$  while recognising that in SESI the reactions occur at atmospheric pressure at partial pressures of water vapour of 1 to 10 mbar. For comparison, typical selected ion flow tube mass spectrometry (SIFT-MS) conditions are  $\sim 1$  mbar total pressure and  $< 0.005$  mbar partial pressure of water vapour. The combination of the experimental and theoretical data explains the substantial difference between the SESI-MS sensitivities of saturated and unsaturated aldehydes. This is a prelude to the studies that are required for other organic compounds.

This article presents and discusses parallel SESI-MS and SIFT-MS analyses of air-containing variables and accurately determined concentrations of saturated and unsaturated aldehyde vapours (C5, pentanal, *trans*-2-pentenal; C7 heptanal, *trans*-2-heptenal; C8, octanal, *trans*-2-octenal). The relative slopes of the SESI-MS calibration curves so obtained are interpreted as the sensitivities for these six compounds, as shown previously.<sup>5</sup> Additionally, the effect of the ion transfer capillary temperature in SESI-MS is characterised. Separate experiments carried out in SIFT-MS with an excessive flow of air containing a variable amount of water vapour were interpreted in terms of rate coefficients of the ligand-switching reactions of the  $\text{H}_3\text{O}^+(\text{H}_2\text{O})_3$  hydrated hydronium ions with the six aldehydes.

Finally, the experimentally observed differences in the reactivity (sensitivity) of the saturated and unsaturated aldehydes are rationally explained by theoretically calculated equilibrium rate constants.

## 2 | METHODS

### 2.1 | SESI-MS

A detailed description of the SESI-MS used in this study is not required, as the major elements are described in our recent paper.<sup>4</sup> It is sufficient to note that a commercial high-efficiency Super SESI X (SSX) SESI-MS ion source (Fossiliontech Madrid, Spain, as detailed in the link <https://www.fossiliontech.com/super-sesi-x>)<sup>12</sup> was used for the present study in combination with a triple stage quadrupole (TSQ) Fortis mass spectrometer (Thermo Fisher Scientific Inc.). The source water was weakly acidified with 0.1% of formic acid to build up the concentration of ions in the solution phase and thus to increase its conductivity to ensure ion current stability at 100 nA as measured by the SSX electronics. The ion spray chamber pressure was held at atmospheric pressure by introducing zero air flow either directly or via a bubble humidifier bottle held at room temperature. The air samples containing the trace amounts of the aldehyde VOCs (taken from the headspace of reference reagents from Sigma Aldrich) were introduced into the chamber at a flow rate of 100 sccm. The atmospheric pressure SESI ion source was linked to the low pressure MS by a heated ion transfer capillary tube held at 250 or 300°C followed by a tube lens (1 mbar pressure, 60 V potential difference), a skimmer and an ion guide (0.1 mbar pressure, 633 V radio frequency voltage) in the standard TSQ Fortis arrangement.

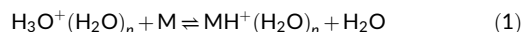
### 2.2 | SIFT-MS

The SIFT-MS analytical technique has been described in numerous publications.<sup>17</sup> The reactions of  $\text{H}_3\text{O}^+$  and its hydrates are the focus of the present studies. Thus,  $\text{H}_3\text{O}^+$  ions were injected into fast-flowing helium carrier gas at a pressure of about 1 Torr and the reactive air/aldehyde mixtures were introduced at a flow rate of 20 sccm. The reagent ions and the product analyte ions were detected by the downstream mass spectrometer operated in the multi-ion monitoring mode, as described previously.<sup>17,18</sup> Note that sampling via a pinhole orifice in Profile 3 is arranged to minimise fragmentation and thus the detected ion count rates directly correspond to the ion concentrations at the end of the flow tube.<sup>19</sup> Concentrations of the aldehydes in the air samples were determined from the known reaction rate coefficients for proton transfer from  $\text{H}_3\text{O}^+$  using the SIFT-MS kinetics library immediately by the Profile 3 data system with an estimated accuracy of  $\pm 20\%$ .<sup>20</sup> Thus, the air/VOC samples flowed simultaneously into both the SIFT-MS helium carrier gas and the SESI-MS chamber, and the calibration for the particular SESI-MS instrument for each of the aldehydes was obtained.

For the SIFT studies of the ligand-switching reactions of the  $\text{H}_3\text{O}^+(\text{H}_2\text{O})_n$  ions, in particular the  $\text{H}_3\text{O}^+(\text{H}_2\text{O})_3$  trihydrate, with the six aldehydes, an additional flow of humid air was introduced into the helium carrier gas at a flow rate of 100 sccm and its humidity was varied from 0 to close to 100% (almost boiling water), allowing full conversion of the injected  $\text{H}_3\text{O}^+$  to its hydrates along the flow tube. A fixed flow rate (10 sccm) of mixtures of the saturated and unsaturated aldehydes ( $\sim 1$  parts per million by volume (ppmv) in clean air) was introduced simultaneously into the helium carrier gas reactor using a T-piece. Variation along the flow tube of the proportions of  $\text{H}_3\text{O}^+$ ,  $\text{H}_3\text{O}^+\text{H}_2\text{O}$ ,  $\text{H}_3\text{O}^+(\text{H}_2\text{O})_2$  and  $\text{H}_3\text{O}^+(\text{H}_2\text{O})_3$  was estimated by modelling the kinetics of the sequence of association reactions of these ions with  $\text{H}_2\text{O}$  and the effective contribution of these ion species to the reactions with aldehydes was estimated by numerical integration (see section 3.3 for more details).

### 2.3 | Quantum chemical calculations

All quantum chemistry calculations were performed using ORCA 5.0.1 software.<sup>21</sup> The molecular geometries of the  $\text{H}_2\text{O}$  molecule and all six neutral aldehyde molecules, their protonated forms and the hydrated ions forms were first drawn using AVOGADRO software<sup>22</sup> and then further optimised using ORCA with the B3LYP density functional theory (DFT) and the basis set 6-311G++(d,p) with the D4 correction.<sup>23</sup> This level of theory was also used to calculate the normal mode vibrational frequencies and thermodynamic quantities of the neutral molecules and ion structures. The total enthalpies of all neutral molecules and ions were thus calculated for standard temperature and pressure (298.15 K, 1 atm). The calculations were performed for several feasible structures of each of the ions and the lowest energy structure was chosen. Enthalpy and entropy changes were calculated for the neutral and ion reactants and the products of the switching reactions:



Equilibrium reaction rate constants were calculated from changes in the Gibbs free energy in these reactions. Polarizabilities and dipole moments were also calculated for the neutral aldehyde molecules using the same DFT method.

## 3 | RESULTS AND DISCUSSION

### 3.1 | SIFT-MS quantification and parallel SESI-MS measurements

A  $\sim 4$ -L Nalophan bag flushed with a continuous flow of air from a Zero air generator was spiked with appropriate concentrations of the three saturated aldehydes and, separately, the three unsaturated aldehydes when coupled simultaneously to the Profile 3 SIFT-MS instrument and to the SESI-MS instrument. Thus, the concentrations

(parts per billion by volume, ppbv) of the aldehydes were accurately measured using Profile 3 SIFT-MS<sup>17,18,20</sup> whilst this mixture also flowed directly into the near atmospheric air surrounding the SESI-MS spray, which was held at 100°C to ensure stable SESI ion currents. Parallel measurements of the response of SESI-MS were made for each of the three aldehydes in the air mixture as the concentrations of the aldehydes were allowed to decrease to near zero by gradually diluting the bag sample by a flow of clean air. The skill of these experiments involved the choice of aldehyde concentrations. The saturated and unsaturated aldehydes had to be investigated separately because of their widely different sensitivities, the unsaturated aldehydes being more than 10 times more sensitive by SESI-MS than the saturated aldehydes, as will be seen later. Four separate experiments were carried out for both the saturated and unsaturated aldehydes for all combinations of two ion transfer capillary temperatures (250 and 300°C) and two humidities (dry, 0.2%, and wet, 1.25% water vapour by volume in air), the humidity being measured by Profile 3.<sup>18,24</sup> The equilibrium distributions of the  $\text{H}_3\text{O}^+(\text{H}_2\text{O})_n$  ions calculated for the present conditions using the same approach as in our previous articles<sup>4,5</sup> exhibit peaks around  $n = 3$  or 4.

The experimental measurements were carried out of the rate coefficients of the reaction of  $\text{H}_3\text{O}^+$  and its hydrates with the aldehydes. The physical parameters of the aldehydes were calculated, viz., their polarizabilities and dipole moments, which are needed to calculate the collisional rate coefficients for their reactions with the reagent ions in SIFT-MS. Estimates of the rate coefficients for the ligand-switching reactions are given in section 3.3. The results of the sensitivities of the aldehydes as measured in SESI-MS are presented next, starting with the three saturated aldehydes.

### 3.1.1 | Saturated aldehydes: pentanal ( $\text{C}_4\text{H}_9\text{CHO}$ ), heptanal ( $\text{C}_6\text{H}_{12}\text{CHO}$ ), octanal ( $\text{C}_7\text{H}_{15}\text{CHO}$ )

To obtain the sensitivities of these aldehydes in SESI-MS, the spectra of primary product (analyte) ions and their hydrates (if any) were obtained as the aldehyde concentration was varied in the SESI chamber. From these quantitative spectra, the peak heights were used to obtain the concentrations of each analyte ion and plotted against the measured concentrations of the aldehydes as measured by SIFT-MS. Concomitantly, as mentioned previously, the water vapour

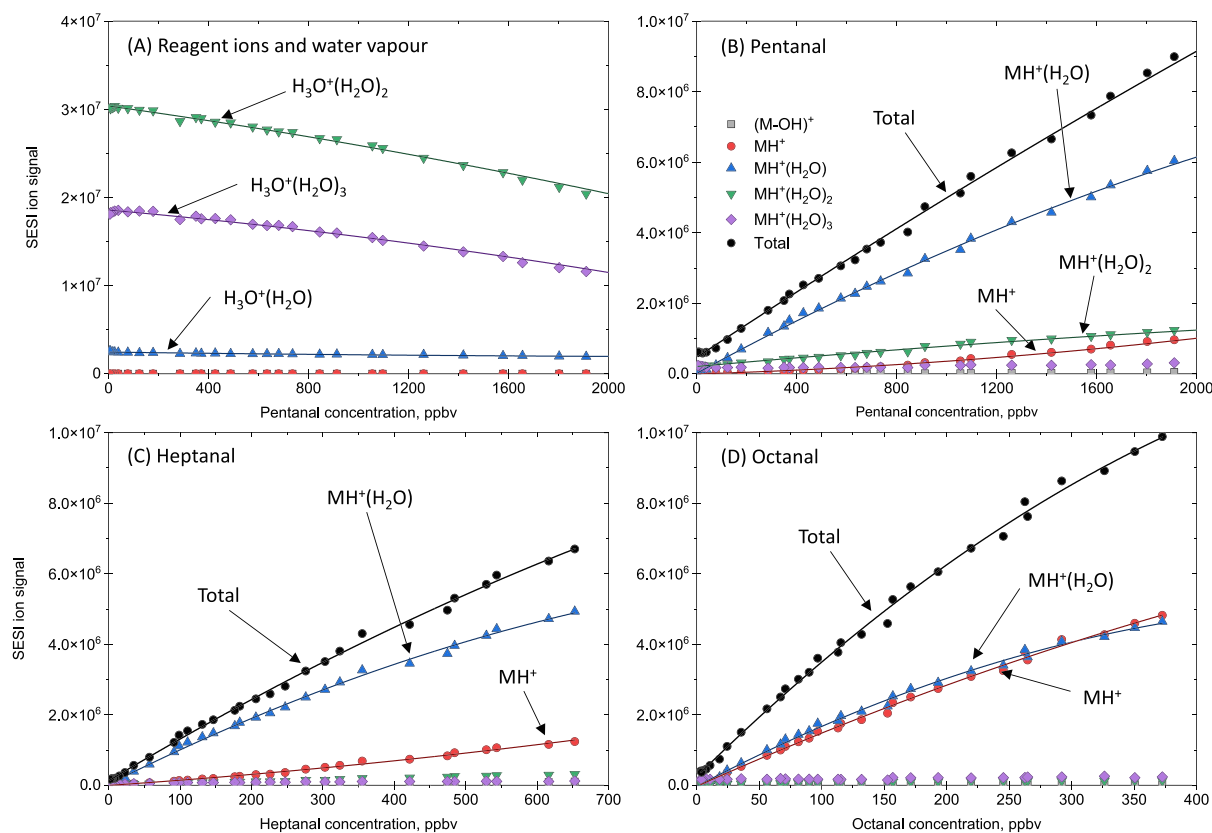
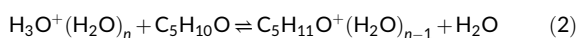


**FIGURE 1** Variations of signals in units given by the MS detection system. (A) The reagent ions and the protonated analyte molecule ions ( $\text{MH}^+$ ) and their hydrates with the concentration of the saturated aldehyde mix in humid SESI support gas ( $\sim 1\%$   $\text{H}_2\text{O}$  by volume) in parts per billion by volume (ppbv), where M is (B) pentanal, (C) heptanal and (D) octanal at an ion transfer capillary temperature of 300°C. The minor ions in all cases are not labelled and the symbols are explained in the legend. [Color figure can be viewed at [wileyonlinelibrary.com](http://wileyonlinelibrary.com)]

in the bag sample was routinely measured by SIFT-MS.<sup>24</sup> These measurements were made for both “dry” and “wet” samples and at two transfer capillary temperatures,  $T$  (250 and 300°C). This produces a large amount of data, therefore we present just the detailed plots of water vapour and the SESI-MS analyte signal levels of the analyte ions for the wet samples at a capillary temperature of 300°C for water vapour ions in Figure 1A and for pentanal in Figure 1B. Note the decreasing signal of the dominant water vapour-related reagent ions at  $m/z$  55 ( $\text{H}_3\text{O}^+(\text{H}_2\text{O})_2$ ) and 73 ( $\text{H}_3\text{O}^+(\text{H}_2\text{O})_3$ ) due to their reaction with the increasing concentration of aldehyde molecules. It should also be noted that 2000 ppbv of pentanal, 600 ppbv of heptanal and 350 ppbv of octanal deplete the reagent ions substantially to two-thirds of the initial signal.

In summary, at a capillary temperature  $T$  of 250°C and dry sample gas,  $m/z$  37 dominates and for wet gas  $m/z$  55 is dominant, with  $m/z$  73 appearing in a significant proportion (37%). At  $T$  of 300°C and dry gas,  $m/z$  19 dominates, and for wet gas,  $m/z$  55 is again dominant and  $m/z$  73 appears at a proportion surprisingly similar to that for 250°C (35%). It is important to note here that the ion signal at  $m/z$  19 ( $\text{H}_3\text{O}^+$ ) is discriminated by about a factor of 10 in the SESI-MS ion detection system, but this has no significant effect on the interpretation of aldehyde sensitivities, which are derived from the plots in Figure 1B for pentanal, and the analogous plots for heptanal and octanal obtained simultaneously in Figure 1C,D.

The plots in Figure 1B show the variations of the product ions recorded by SESI-MS as a function of the bag sample concentration as recorded by the parallel measurements by SIFT-MS. Note that the major product is at  $m/z$  105, which is the monohydrate of protonated pentanal at  $m/z$  87. This major product ion is formed by the switching reactions of the reagent  $\text{H}_3\text{O}^+$  hydrates with the pentane molecule and the dihydrate, and a very small fraction of the trihydrate ions is also formed in these switching reactions:



Note the close-to-linearity of these plots, which is also the case for the analogous heptanal and octanal plots. It is significant that a small fraction of the fragment ion appears at  $m/z$  69,  $\text{C}_5\text{H}_9^+$ , resulting from the loss of an  $\text{H}_2\text{O}$  molecule from the small fraction of protonated pentane at  $m/z$  87, herewith designated  $\text{MH}^+$  for all the aldehydes for simplicity, which implies that a small fraction of  $\text{H}_3\text{O}^+$

ions is present as a reagent ion in the atmospheric pressure region and/or in the transfer capillary since the switching reaction does not produce the fragment resulting from the  $\text{H}_3\text{O}^+$ /pentanal reaction.<sup>25,26</sup> Note also that in the dry situation, the fragment ion at  $m/z$  69,  $\text{C}_5\text{H}_9^+$ , dominates and is three times more intense than  $\text{MH}^+$ . A small fraction of the fragment at  $m/z$  97 also appears in the spectrum for the heptanal, C7, but the second hydrate,  $\text{MH}^+(\text{H}_2\text{O})_2$ , is smaller than for pentanal, C5. There is visibly less fragmentation ( $m/z$  111) for octanal, C8, and a smaller fraction of the monohydrate ( $m/z$  147). It is important to note again that the experiments were carried out using a mixture of the three saturated (and three unsaturated subsequently) aldehydes, thus the conditions were the same for these saturated and unsaturated aldehyde reactions and direct comparisons are quite valid. This does not take into account the possibility of analytes competing for charge in situations where the reagent ion concentrations are depleted.

The slopes of these plots provide the relative SESI-MS sensitivity for these saturated aldehydes as the SESI-MS signal level per ppbv. Further discussion of this is given in our previous paper,<sup>5</sup> which alerted us to the much greater sensitivity,  $S$ , for the unsaturated aldehydes, as described in the next section. The derived sensitivities for both the dry and wet samples and at the two capillary temperatures for the six aldehydes are listed in Table 1, and for the three unsaturated aldehydes, as discussed in the next subsection. The trend with the number of C atoms, C5, C7 and C8, in the aldehydes is consistent for the four experiments  $S(\text{C8}) > S(\text{C7}) > S(\text{C5})$ . The dry sample sensitivities are greater than the wet sample sensitivities. This could be due to the presence of a fraction of  $\text{H}_3\text{O}^+$  or its smaller hydrates, as suggested previously regarding fragment ion production. Additionally, in the wet samples, the fractions of higher-order hydrated  $\text{H}_3\text{O}^+$  are greater (greater  $n$ , see Equation 1), indicating that the unsaturated aldehydes react slowly or not at all by switching with the hydrated hydronium reagent ions. At the higher capillary temperature, the situation is further complicated by the increased desolvation of both reagent and analyte ions and the likely production of small fractions of  $\text{H}_3\text{O}^+$  resulting in lower sensitivities for switching with the  $\text{H}_3\text{O}^+$  hydrates and more proton transfer from  $\text{H}_3\text{O}^+$  to the aldehydes. These observations show that the actual setup of the SESI-MS (capillary length and temperature) will have a profound effect on the sensitivities (and relative sensitivities) to these aldehydes and other compounds.

**TABLE 1** The net sensitivities (total signal of product ions versus ppbv) in units of  $10^3$ /ppbv.

Compound	Dry 250 °C	Dry 300 °C	Wet 250 °C	Wet 300 °C
Pentanal	36	45	12	5
Heptanal	72	56	26	11
Octanal	78	62	56	30
2-pentenal	276	151	606	313
2-heptenal	437	259	1,280	473
2-octenal	603	716	1,650	774

### 3.1.2 | Unsaturated aldehydes: 2-pentenal $C_2H_5CH=CHCHO$ , 2-heptenal $C_4H_9CH=CHCHO$ , 2-octenal $C_7H_{11}CH=CHCHO$

The experimental approach taken is identical to that described for the saturated aldehydes. The three unsaturated aldehydes (all in the *trans* conformation) were present in the sample bag, which was coupled to both the SIFT-MS and SESI-MS instruments simultaneously. Again, four separate experiments were carried out, as for the saturated aldehydes, at two ion transfer capillary temperatures (250 and 300°C) and for dry and wet sample gas. The major difference was that the saturated aldehyde concentrations were at a level of a few hundred ppbv (see Figure 1) whereas that for the unsaturated aldehydes were at a level of a few tens of ppbv, as can be seen in Figure 2, which was obtained for wet sample gas and a capillary temperature of 300°C. This was necessary because of the much greater reactivity of the unsaturated aldehydes with the  $H_3O^+$  hydrates. Thus, at the concentration used for the more slowly reacting saturated aldehydes the unsaturated aldehydes greatly reduce the reagent ions to unworkable levels. Even at the lower concentration, the plots of SESI-MS signal versus the SIFT-MS measured concentration depart from linearity. As can be seen in Figure 2B, even 60 ppbv of

2-pentenal together with the other aldehydes is sufficient to reduce the reagent ions by three times. Compare this with Figure 1B, where 2000 ppbv caused little departure from linearity. The sensitivities for these three unsaturated aldehydes were therefore obtained from the slopes of the total product ion signals in the linear lower concentrations part of the plots, as given in Table 1.

Some minor ion fragments are again observed for unsaturated aldehydes, resulting from the loss of an  $H_2O$  molecule from the protonated aldehyde, implying that a small fraction of  $H_3O^+$  ions are present in the SESI ion source, mostly when using the dry sample gas, and perhaps produced by desolvation in the heated transfer capillary. The spectra for 2-heptenal and 2-octenal (see Figure 2C,D) show fragment ions at  $m/z$  95 and 109 due to loss of  $H_2O$  from  $MH^+$  (note that this fragmentation does not occur in truly thermal SIFT<sup>27</sup>), which is present even for wet samples (in contrast to saturated octanal). In general, there is less hydration of the product ions and only the first hydrate  $MH^+H_2O$  is significant.

With reference to Table 1, it can be seen that SESI-MS is much more sensitive to the unsaturated aldehydes for all conditions of wet/dry samples and at both capillary temperatures. Again, the trend with the number of C atoms in the aldehydes is consistent for unsaturated aldehydes in all four experiments  $S(C8) > S(C7) > S(C5)$ .

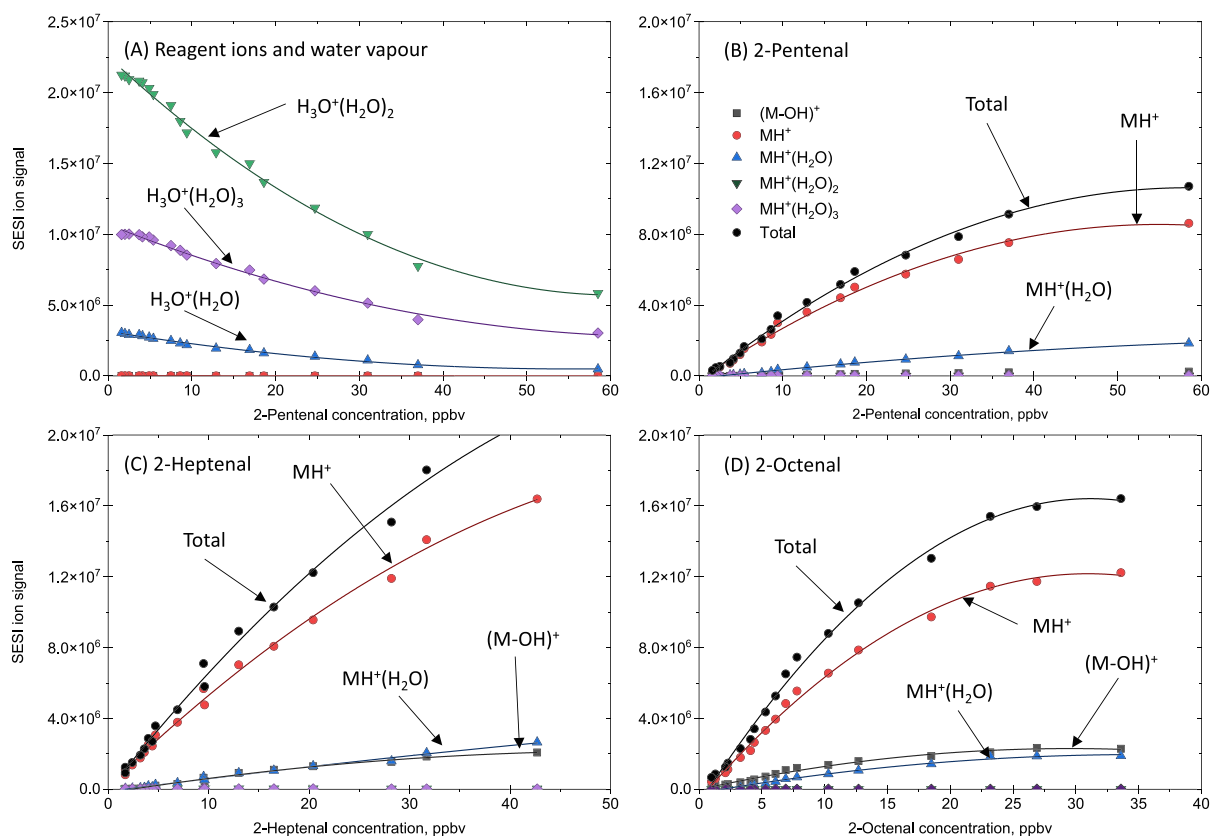


**FIGURE 2** Variations of signals in units given by the MS detection system. (A) The reagent ions and the protonated analyte molecule ions ( $MH^+$ ), their hydrates and associated fragment ions  $(M-OH)^+$  with the concentration of the unsaturated aldehyde mix in humid SESI support gas ( $\sim 1\%$   $H_2O$  by volume) in parts per billion by volume (ppbv), where M is (B) 2-pentenal, (C) 2-heptenal and (D) 2-octenal at an ion transfer capillary temperature of 300°C. [Color figure can be viewed at [wileyonlinelibrary.com](http://wileyonlinelibrary.com)]

However, the dry gas sensitivity for all three unsaturated compounds is lower than the wet gas sensitivity. A possible reason for this is the greater diffusion losses of  $MH^+$  in comparison to hydrates. It cannot be overstated that this substantial difference in sensitivity between the saturated and unsaturated aldehydes needs to be understood if SESI-MS is to be used for quantitative analyses. This difference is also apparent for other volatile organic compounds, as indicated in our previous paper.<sup>5</sup> Why should there be such large differences? Clearly, it is the different ion chemistries occurring in the SESI ions. In the next section, we discuss this chemistry in terms of the differing physical parameters of the reactant (analyte) molecules, the kinetic of the reactions and the thermochemistry.

### 3.2 | Ligand-switching reaction: energetics and kinetics

The proton affinities for the six aldehydes and thermochemical values for the reactions (1) for the number of hydrating  $H_2O$  molecules,  $n$ , in the range from 1 to 3 are given in Table 2.

These data show that whilst all the reactions are exergonic (negative  $\Delta G$ ) and exothermic (negative  $\Delta H$ ), there is a clear decreasing trend in these values with the number of solvating  $H_2O$  molecules. Additionally, the exergonicity is systematically lower for saturated aldehyde reactions compared to their unsaturated counterparts. Note that the reactions of  $H_3O^+(H_2O)_3$  are close to

thermoneutral and thus can reach equilibrium ( $K$  of order 10) in the presence of  $H_2O$  molecules with a much smaller concentration of the product ions.

The maximum rate coefficient for the exothermic switching reaction is the gas kinetic (or collisional) rate (coefficient  $k_c$ ) as calculated by the method of Su and Chesnavich.<sup>28</sup> The calculation requires the polarizability,  $\alpha$ , and dipole moment,  $D$ , of the reactive aldehyde molecule. These were calculated using DFT, as explained in Section 2.3. The values of  $\alpha$  and  $D$ , and the derived  $k_c$  for the reaction of  $H_3O^+$  with all the VOCs included are given in Table 3. Note that the  $k_c$  values are quite large, especially for the unsaturated aldehydes, principally due to their large dipole moments (Table 3).

### 3.3 | SIFT studies of the reactions of $H_3O^+(H_2O)_3$ with saturated and unsaturated aldehydes

The  $H_3O^+(H_2O)_3$  ions were formed in the SIFT by a sequence of ternary association reactions of the injected  $H_3O^+$  ions with  $H_2O$  molecules mediated by the helium carrier gas atoms and air molecules. Air at a flow rate of 100 sccm (four times greater than used for SIFT-MS) was introduced at variable humidity from 0 to near 100% to achieve a concentration of  $H_2O$  ( $[H_2O]$ ) that was sufficient for full conversion of  $H_3O^+$  to their hydrated ions. The reaction time,  $t_r$ , was 0.37 ms, the maximum number density of  $H_2O$  molecules in the flow tube was  $2 \times 10^{15} \text{ cm}^{-3}$  and the He carrier gas number

**TABLE 2** Proton affinities (PA), enthalpy changes ( $\Delta H$ ), Gibbs free energy changes ( $\Delta G$ ) and equilibrium constants ( $K$ ) calculated for the ligand-switching reaction (1) for  $n = 1$  to 3 at  $T = 298.15 \text{ K}$ .

Aldehyde M	PA (kJ/mol)	$n = 1$			$n = 2$			$n = 3$		
		$\Delta H$ (kJ/mol)	$\Delta G$ (kJ/mol)	$K$	$\Delta H$ (kJ/mol)	$\Delta G$ (kJ/mol)	$K$	$\Delta H$ (kJ/mol)	$\Delta G$ (kJ/mol)	$K$
Pentanal	791	-53	-48	$2 \times 10^8$	-31	-20	$3 \times 10^3$	-18	-7	14
Heptanal	793	-54	-49	$3 \times 10^8$	-31	-20	$3 \times 10^3$	-18	-7	16
Octanal	793	-54	-49	$3 \times 10^8$	-31	-20	$3 \times 10^3$	-18	-7	15
2-pentenal	844	-88	-83	$10^{14}$	-55	-45	$7 \times 10^8$	-35	-24	$10^4$
2-heptenal	854	-98	-92	$10^{16}$	-63	-52	$10^9$	-42	-30	$2 \times 10^5$
2-octenal	851	-93	-87	$10^{15}$	-59	-47	$2 \times 10^8$	-37	-26	$3 \times 10^4$

**TABLE 3** Polarizability ( $\alpha$ ) and dipole moments ( $D$ ) of the aldehyde molecules used for the calculation of ion-molecule collisional rate coefficients ( $k_c$ ).

Aldehyde	Formula	MW	$\alpha$ ( $\text{\AA}^3$ )	$D$ (Debye)	$k_c$ ( $10^{-9} \text{ cm}^3 \text{ s}^{-1}$ )			
					$m/z$ 19	$m/z$ 37	$m/z$ 55	$m/z$ 73
Pentanal	$C_5H_{10}O$	86	9.6	2.83	3.92	3.04	2.67	2.46
Heptanal	$C_7H_{14}O$	114	13.3	2.84	4.04	3.09	2.68	2.45
Octanal	$C_8H_{16}O$	128	15.1	2.76	4.10	3.11	2.69	2.44
2-pentenal	$C_5H_8O$	84	10.2	4.39	5.50	4.28	3.76	3.47
2-heptenal	$C_7H_{12}O$	112	14.0	4.57	5.75	4.39	3.81	3.48
2-octenal	$C_8H_{14}O$	126	15.6	4.49	5.70	4.33	3.74	3.41

Abbreviation: MW, molecular weight.

density was  $3.6 \times 10^{16} \text{ cm}^{-3}$ . The observed experimental dependence of the  $\text{H}_3\text{O}^+(\text{H}_2\text{O})_{0-3}$  reagent ion count rate observed at the end of the SIFT reactor by the mass spectrometer/detection system on the  $\text{H}_2\text{O}$  concentration is shown in Figure 3.

Whilst the plots in Figure 3 are obtained for a fixed  $t_r$  and variable  $[\text{H}_2\text{O}]$ , they could be effectively interpreted as dependencies on variable  $t_r$  for the fixed humidity  $[\text{H}_2\text{O}]$  because it is the product of these two variables  $t_r[\text{H}_2\text{O}]$  that governs the reaction kinetics. Thus, the plot for  $n=0$  shows how the  $\text{H}_3\text{O}^+$  ion concentration reduces with time along the flow tube. We can therefore use it to estimate the contributions of each of the ions  $\text{H}_3\text{O}^+(\text{H}_2\text{O})_n$  to the reactions with the aldehyde molecules. Numerical integration of the areas under the curves gives the following relative contributions:  $\text{H}_3\text{O}^+$  (0.18),  $\text{H}_3\text{O}^+\text{H}_2\text{O}$  (0.08);  $\text{H}_3\text{O}^+(\text{H}_2\text{O})_2$  (0.18);  $\text{H}_3\text{O}^+(\text{H}_2\text{O})_3$  (0.60) and only 0.01 for  $\text{H}_3\text{O}^+(\text{H}_2\text{O})_4$ . Even though the ion signal at  $m/z$  19 is

negligible downstream,  $\text{H}_3\text{O}^+$  still amounts to a 0.18 fraction of the reagent ions, on average, along the flow tube. A fixed flow rate of a mixture of a saturated and an unsaturated aldehyde independently was introduced at a flow rate of 10 sccm and the variation of the signal intensities of the product ions of their reactions with  $\text{H}_3\text{O}^+$  and their hydrates were recorded as a function of  $[\text{H}_2\text{O}]$ . The data obtained for the C7 aldehydes are shown in Figure 4.

Note that at an x-axis value of 0, we see the products of mostly the  $\text{H}_3\text{O}^+$  reactions (see Figure 3). As the humidity increases and the reagent ion composition shifts towards  $m/z$  73, the total signal for the heptanal product ions (black line in Figure 4A) decreases by a greater fraction than the corresponding total signal for the 2-heptenal product ions (Figure 4B). Numerical fitting of the experimental data using the above estimated contributions of the  $\text{H}_3\text{O}^+(\text{H}_2\text{O})_{0-4}$  reagent ions with the rate coefficients of their reactions with M as the

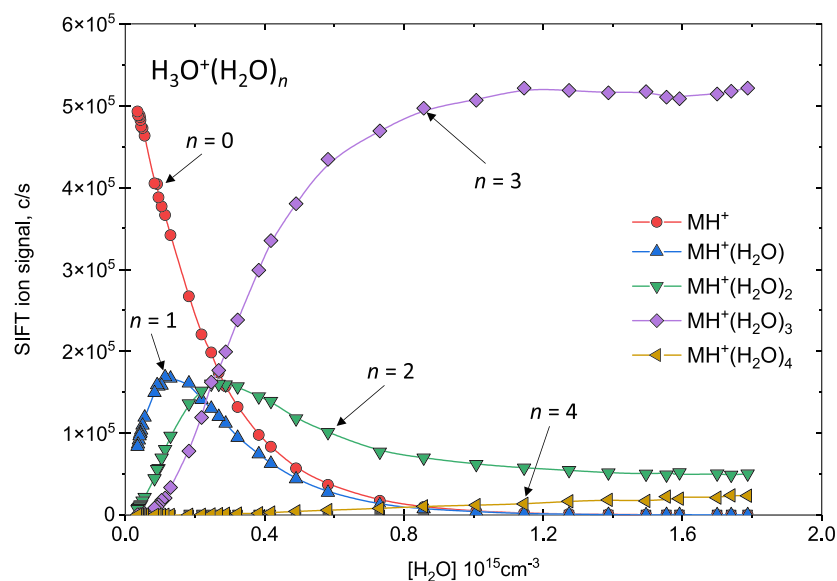


**FIGURE 3** The detected signal of the  $\text{H}_3\text{O}^+(\text{H}_2\text{O})_{0-4}$  ions in counts per second (c/s) as a function of the number density of water molecules ( $[\text{H}_2\text{O}]$ ) in the SIFT reactor. Note that at the highest  $[\text{H}_2\text{O}]$ ,  $m/z$  73 becomes the dominant ion whilst the  $\text{H}_3\text{O}^+$  signal reduces by six orders of magnitude to below 1 c/s. [Color figure can be viewed at [wileyonlinelibrary.com](https://onlinelibrary.wiley.com/terms-and-conditions)]

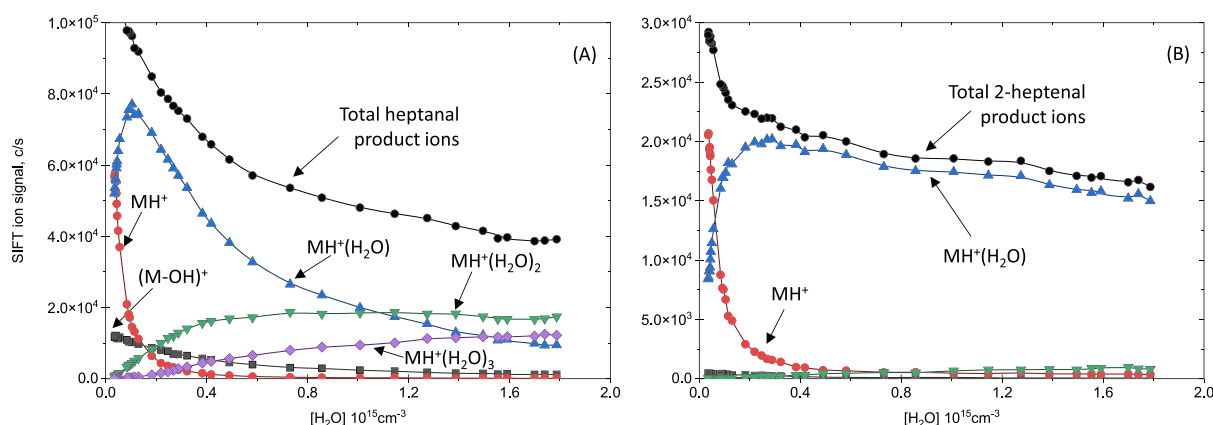


**FIGURE 4** The dependencies of the count rates of the  $(\text{M}-\text{OH})^+$  and  $\text{MH}^+(\text{H}_2\text{O})_{0-3}$  ions on the water vapour number density ( $[\text{H}_2\text{O}]$ ) for (A) heptanal and (B) 2-heptenal. [Color figure can be viewed at [wileyonlinelibrary.com](https://onlinelibrary.wiley.com/terms-and-conditions)]

**TABLE 4** Experimentally estimated rate coefficients for the reactions of  $\text{H}_3\text{O}^+$  ( $k_{19}$ ) and those for  $\text{H}_3\text{O}^+(\text{H}_2\text{O})_3$  ( $k_{73}$ ) and its collisional rate coefficient ( $k_{c73}$ ) with the aldehyde molecules.

Aldehyde	$k_{19}$ , $\text{H}_3\text{O}^{\text{a}}$	$k_{73}$ , $\text{H}_3\text{O}^+(\text{H}_2\text{O})_3$	$k_{c73}$	$k_{73}/k_{c73}$
Pentanal	3.9	0.8	(2.5)	0.33
Heptanal	4.0	0.6	(2.5)	0.25
Octanal	4.1	0.6	(2.5)	0.25
2-pentenal	5.5	3.5	(3.5)	1
2 heptenal	5.8	3.5	(3.5)	1
2 octenal	5.7	3.4	(3.4)	1

<sup>a</sup> $k_{19}$  is equal to the corresponding collisional rate coefficient  $k_{c19}$  in all six cases.

free parameter provided estimates of the rate coefficients of the  $m/z$  19  $\text{H}_3\text{O}^+$  ion reactions,  $k_{19}$ , and of the  $m/z$  73  $\text{H}_3\text{O}^+(\text{H}_2\text{O})_3$  ion reactions,  $k_{73}$ , which are given in Table 4 together with the calculated  $\text{H}_3\text{O}^+(\text{H}_2\text{O})_3$  collisional rate coefficients  $k_{c73}$ .

The results clearly indicate that the  $m/z$  73 reactions with the saturated aldehydes are significantly slower than for the unsaturated aldehydes. This is in line with the equilibrium constants from the thermochemistry calculations, which predict that reverse reactions of the products of ligand switching  $\text{MH}^+(\text{H}_2\text{O})_3$  will take place, effectively slowing down the forward reactions.

## 4 | SUMMARY AND CONCLUDING REMARKS

The major objective of this study was to explain why the detection sensitivity in SESI-MS of unsaturated aldehydes was much greater than for saturated aldehydes, as observed in recent previous studies. This is not a marginal difference. SESI-MS experiments using an SSX commercial source showed that the sensitivities for the unsaturated aldehydes are 25 to 62 times greater than for saturated aldehydes as long as the atmospheric source support gas of the SESI source is humid (wet). This is also confirmed by previous ZSpray experiments. However, when the source support gas is relatively dry, the sensitivities for unsaturated aldehydes are still higher but now only by 3 to 12 times than those for saturated aldehydes. In short, increased humidity increases the sensitivity to unsaturated aldehydes, whilst it decreases the sensitivity to saturated aldehydes. This trend, coupled with the observation that an increase in the minor signal of fragment ions ( $\text{M-OH}^+$ ) is apparent at lower humidity, indicates that ligand switching dominates at higher humidity, whereas proton transfer may take place at low humidity.

For clarification, standard conditions for SSX SESI-MS are humid samples and a 250°C transfer capillary temperature; under these conditions, the reagent ions are predominantly  $n = 3$  and 4. However, in very dry conditions, smaller reagent ions appear,  $n = 0$ , and some fragmentation can take place. For example, unsaturated aldehydes in truly thermal (really “soft”) SIFT-MS do produce fragments in

reactions with  $\text{H}_3\text{O}^+$ . In SESI, the fragmentation presumably can occur in the heated transfer capillary and in the tube lens, which acts as a drift tube with 60 V across  $\sim 1$  cm at  $\sim 1$  mbar pressure ( $N = 2 \times 10^{16}$   $\text{cm}^{-3}$ ), equating to an  $E/N$  of 200 Td. In air, this can elevate the ion-molecule collisional energy well above thermal. Similar fragmentation was observed in SESI-MS with Orbitrap MS, but with somewhat different ion optics following the ion transfer capillary.<sup>9</sup>

To substantiate these deductions, SIFT experiments were carried out to investigate the kinetics of the reactions of  $\text{H}_3\text{O}^+(\text{H}_2\text{O})_{0-4}$  with the aldehydes. Thus, the low sensitivity to saturated aldehydes can be explained by the observed kinetics of the ligand-switching reactions of the  $\text{H}_3\text{O}^+$  hydrates, which reveal that the observed  $k_{73}$  values are three to four times slower for saturated than for unsaturated aldehydes. Calculated equilibrium constants,  $K$ , favour the reverse reactions, with  $\text{H}_2\text{O}$  effectively slowing down the formation of the analyte ions. The number density of  $\text{H}_2\text{O}$  molecules in SESI support gas is always orders of magnitude greater than that of the trace analyte molecules, so the reverse reactions will be much faster when  $K$  is in the order of 10 to 100.

This paper discusses only the relative SESI-MS sensitivities to saturated and unsaturated aldehydes, but our previous paper indicated that such differences occur for other volatile organic compounds, being totally insensitive to some hydrocarbons. The present experimental study has cast light on the central role ligand switching plays in SESI ion chemistry, which is supported and rationally explained by theoretically calculated equilibrium rate constants derived from thermochemical DFT calculations of free energy changes in the ligand exchange reactions as the  $\text{H}_2\text{O}$  number density is varied in the SESI atmospheric support gas. Nevertheless, further work is needed before the underlying chemistry of this technique is understood and can be used with confidence for quantitative gas-phase trace gas analysis.

## ACKNOWLEDGMENTS

We acknowledge funding from the Czech Science Foundation GACR (project number 21-25486S) and the Praemium Academiae award by the Czech Academy of Sciences. We thank Miroslav Polášek for useful discussions and ideas for further experiments.

## DATA AVAILABILITY STATEMENT

The data that support the findings of this study are available from the corresponding author upon reasonable request.

## ORCID

Patrik Španěl  <https://orcid.org/0000-0002-9868-8282>

Kseniya Dryahina  <https://orcid.org/0000-0003-4247-3642>

Maroua Omezzine Gnioua  <https://orcid.org/0000-0003-1096-915X>

David Smith  <https://orcid.org/0000-0002-7860-9452>

## PEER REVIEW

The peer review history for this article is available at <https://publons.com/publon/10.1002/rcm.9496>.

## REFERENCES

- Martínez-Lozano Sinues P, Rus J, Fernández de la Mora G, Hernández M, Fernández de la Mora J. Secondary electrospray ionization (SESI) of ambient vapors for explosive detection at concentrations below parts per trillion. *J Am Soc Mass Spectrom.* 2009;20(2):287-294. doi:10.1016/j.jasms.2008.10.006
- Dillon LA, Stone VN, Croasdell LA, Fielden PR, Goddard NJ, Paul Thomas CL. Optimisation of secondary electrospray ionisation (SESI) for the trace determination of gas-phase volatile organic compounds. *Analyst.* 2010;135(2):306-314. doi:10.1039/b918899a
- Rioseras AT, Gaugg MT, Martínez-Lozano Sinues P. Secondary electrospray ionization proceeds via gas-phase chemical ionization. *Anal Methods.* 2017;9(34):5052-5057. doi:10.1039/C7AY01121K
- Dryahina K, Som S, Smith D, Španěl P. Reagent and analyte ion hydrates in secondary electrospray ionization mass spectrometry (SESI-MS), their equilibrium distributions and dehydration in an ion transfer capillary: Modelling and experiments. *Rapid Commun Mass Spectrom.* 2021;35(7):e9047. doi:10.1002/rcm.9047
- Dryahina K, Poláček M, Smith D, Španěl P. Sensitivity of secondary electrospray ionization mass spectrometry to a range of volatile organic compounds: Ligand switching ion chemistry and the influence of Zspray™ guiding electric fields. *Rapid Commun Mass Spectrom.* 2021;35(22):e9187. doi:10.1002/rcm.9187
- Spesvyvi A, Lacko M, Dryahina K, Smith D, Španěl P. Ligand switching ion chemistry: An SIFT-MS case study of the primary and secondary reactions of protonated acetic acid hydrates with acetone. *J Am Soc Mass Spectrom.* 2021;32(8):2251-2260. doi:10.1021/jasms.1c00174
- Martínez-Lozano Sinues P, Criado E, Vidal G. Mechanistic study on the ionization of trace gases by an electrospray plume. *Int J Mass Spectrom.* 2012;313:21-29. doi:10.1016/j.ijms.2011.12.010
- de la Mora JF. Ionization of vapor molecules by an electrospray cloud. *Int J Mass Spectrom.* 2011;300(2-3):182-193. doi:10.1016/j.ijms.2010.09.009
- Kaeslin J, Wuthrich C, Giannoukos S, Zenobi R. How soft is secondary electrospray ionization? *J Am Soc Mass Spectrom.* 2022;33(10):1967-1974. doi:10.1021/jasms.2c00201
- Liu C, Zeng J, Sinues P, Fang M, Zhou Z, Li X. Quantification of volatile organic compounds by secondary electrospray ionization-high resolution mass spectrometry. *Anal Chim Acta.* 2021;1180:338876. doi:10.1016/j.aca.2021.338876
- Martínez-Lozano Sinues P, de la Mora JF. Electrospray ionization of volatiles in breath. *Int J Mass Spectrom.* 2007;265(1):68-72. doi:10.1016/j.ijms.2007.05.008
- Lan J, Kaeslin J, Greter G, Zenobi R. Minimizing ion competition boosts volatile metabolome coverage by secondary electrospray ionization orbitrap mass spectrometry. *Anal Chim Acta.* 2021;1150:338209. doi:10.1016/j.aca.2021.338209
- Midey AJ, Williams S, Arnold ST, Viggiano AA. Reactions of  $\text{H}_3\text{O}^+(\text{H}_2\text{O})_{(0,1)}$  with alkylbenzenes from 298 to 1200 K. *J Phys Chem a.* 2002;106(48):11726-11738. doi:10.1021/jp014141e
- Španěl P, Smith D. Reactions of hydrated hydronium ions and hydrated hydroxide ions, with some hydrocarbons and oxygen-bearing organic-molecules. *J Phys Chem.* 1995;99(42):15551-15556. doi:10.1021/j100042a033
- Viggiano AA, Dale F, Paulson JF. Proton transfer reactions of  $\text{H}^+(\text{H}_2\text{O})_{n=2-11}$  with methanol, ammonia, pyridine, acetonitrile, and acetone. *J Chem Phys.* 1988;88(4):2469-2477. doi:10.1063/1.454027
- Španěl P, Smith D. Selected ion flow tube mass spectrometry analyses of stable isotopes in water: Isotopic composition of  $\text{H}_3\text{O}^+$  and  $\text{H}_3\text{O}^+(\text{H}_2\text{O})_{(3)}$  ions in exchange reactions with water vapor. *J Am Soc Mass Spectrom.* 2000;11(10):866-875. doi:10.1016/S1044-0305(00)00157-4
- Španěl P, Smith D. Progress in SIFT-MS: Breath analysis and other applications. *Mass Spectrom Rev.* 2011;30(2):236-267. doi:10.1002/mas.20303
- Španěl P, Smith D. Advances in on-line absolute trace gas analysis by SIFT-MS. *Curr Anal Chem.* 2013;9(4):525-539. doi:10.2174/15734110113099990017
- Smith D, Pysanenko A, Španěl P. Ionic diffusion and mass discrimination effects in the new generation of short flow tube SIFT-MS instruments. *Int J Mass Spectrom.* 2009;281(1-2):15-23. doi:10.1016/j.ijms.2008.11.007
- Španěl P, Dryahina K, Smith D. A general method for the calculation of absolute trace gas concentrations in air and breath from selected ion flow tube mass spectrometry data. *Int J Mass Spectrom.* 2006;249:230-239. doi:10.1016/j.ijms.2005.12.024
- Neese F. Software update: The ORCA program system, version 4.0. *Wiley Interdiscip Rev Comput Mol Sci.* 2018;8(1). doi:10.1002/wcms.1327
- Hanwell MD, Curtis DE, Lonie DC, Vandermeersch T, Zurek E, Hutchison GR. Avogadro: An advanced semantic chemical editor, visualization, and analysis platform. *J Chem.* 2012;4(1):17. doi:10.1186/1758-2946-4-17
- Caldeweyher E, Bannwarth C, Grimme S. Extension of the D3 dispersion coefficient model. *J Chem Phys.* 2017;147(3):034112. doi:10.1063/1.4993215
- Španěl P, Smith D. On-line measurement of the absolute humidity of air, breath and liquid headspace samples by selected ion flow tube mass spectrometry. *Rapid Commun Mass Spectrom.* 2001;15(8):563-569. doi:10.1002/rcm.265
- Smith D, Chippendale TWE, Španěl P. Reactions of the selected ion flow tube mass spectrometry reagent ions  $\text{H}_3\text{O}^+$  and  $\text{NO}^+$  with a series of volatile aldehydes of biogenic significance. *Rapid Commun Mass Spectrom.* 2014;28(17):1917-1928. doi:10.1002/rcm.6977
- Španěl P, Ji YF, Smith D. SIFT studies of the reactions of  $\text{H}_3\text{O}^+$ ,  $\text{NO}^+$  and  $\text{O}_2^+$  with a series of aldehydes and ketones. *Int J Mass Spectrom.* 1997;165:25-37. doi:10.1016/S0168-1176(97)00166-3
- Španěl P, Van Doren JM, Smith D. A selected ion flow tube study of the reactions of  $\text{H}_3\text{O}^+$ ,  $\text{NO}^+$ , and  $\text{O}_2^+$  with saturated and unsaturated aldehydes and subsequent hydration of the product ions. *Int J Mass Spectrom.* 2002;213(2-3):163-176. doi:10.1016/S1387-3806(01)00531-0
- Su T, Chesnavich WJ. Parametrization of the ion-polar molecule collision rate constant by trajectory calculations. *J Chem Phys.* 1982;76(10):5183-5185. doi:10.1063/1.442828

**How to cite this article:** Španěl P, Dryahina K, Omezzine Gnioua M, Smith D. Different reactivities of  $\text{H}_3\text{O}^+(\text{H}_2\text{O})_n$  with unsaturated and saturated aldehydes: ligand-switching reactions govern the quantitative analytical sensitivity of SESI-MS. *Rapid Commun Mass Spectrom.* 2023;37(9):e9496. doi:10.1002/rcm.9496